Original Article
Engrafted peripheral blood-derived mesenchymal stem cells promote locomotive recovery in adult rats after spinal cord injury

Qiang Fu[1,2,3], Yi Liu[2], Xiu Liu[1], Qian Zhang[4], Long Chen[1,5], Jiachen Peng[2], Jun Ao[2], Yuwan Li[2], Shengmin Wang[2], Gongyu Song[4], Limei Yu[1], Jinwei Liu[1], Tao Zhang[1]

[1]Key Laboratory of Cell Engineering of Guizhou Province and Regenerative Medicine Centre, Affiliated Hospital of Zunyi Medical College; Zunyi, Guizhou, China; [2]Department of Orthopedics, Affiliated Hospital of Zunyi Medical College, Zunyi, Guizhou, China; [3]Sichuan Academy of Medical Sciences and Sichuan Provincial People's Hospital, School of Medicine, University of Electronic Science and Technology of China, Chengdu, Sichuan, China; [4]Department of Human Anatomy, Zunyi Medical College, Zunyi, Guizhou, China; [5]Experimental Centre, Affiliated Dongfeng General Hospital of Hubei University of Medicine, Shiyan, Hubei, China

Abstract: Spinal cord injury (SCI) is a severe trauma of central nervous system (CNS). Numerous stem cells have been applied for SCI therapy. Peripheral blood-derived mesenchymal stem cells (PBMSCs) have captured researchers' attention by virtue of pluripotency and effectiveness. However, little work has been performed on whether PBMSCs play roles and what role, if any, in the lesion microenvironment. Through the investigation of the differentiation, neuroprotection and immunoloregulation of engrafted PBMSCs, we found that the expression of glial fibrillary acidic protein (GFAP) was inhibited. Meanwhile, myelin basic protein (MBP), neurofilament protein-200 (NF-200) and microtubule associated protein-2 (MAP-2) were promoted after PBMSC transplantation (PBMSCT) by immunohistochemistry. Though engrafted PKH26+PBMSCs could survive in vivo for at least 8 w, they could not respectively express GFAP, MBP and neuronal specific neucleoprotein (NeuN) by immunofluorescence. Additionally, Flow cytometry demonstrated that the number of CD4+IL17+Th17 cells decreased while CD4+CD25+Foxp3+Treg ones increased after PBMSCT ($P < 0.01$). Immunohistochemistry and Elisa both showed a lower expression of IL-6 and IL-17a while a higher expression of TGF-β after PBMSCT ($P < 0.05$). RT-PCR indicated that Th17-relevant genes including RORγT, IL-6 and IL-21 were inhibited and resulted in the decrease of IL-23a and IL-22 secretion ($P < 0.05$); Treg-relevant genes including FoxP3 and TGF-β and the secretion of IL-10 were improved ($P < 0.05$). Accordingly, we concluded that the PBMSCT-relevant therapy took effect not through the differentiation of PBMSCs into CNS cells, but through regulating Th17/Treg-relevant gene expression, inhibiting Th17-relevant gene expression and meanwhile promoting Treg-relevant gene expression, and eventually resulted in promotion of the functional recovery of SCI rats.

Keywords: Peripheral blood, mesenchymal stem cells (MSCs), spinal cord injury (SCI), cell transplantation, immunoloregulation, rats

Introduction

Spinal cord injury (SCI), a severe trauma often caused by car accidents or falls, usually induces loss of autonomic function and/or sensation below the level of injury [1]. It presents a high incidence, high morbidity, huge cost and lowering trend of age. SCI therapy conventionally includes methylprednisolone or/and surgery. However the situation has not been substantially improved yet. Additionally, methylprednisolone pulse therapy may increase rates of respiratory infection and hyperglycaemia *etc.*, which usually lengthens hospital stay [2]. Though surgery can relieve spinal cord compression and restore the stability of spinal column, a secondary injury could not be relieved. It may eventually result in the loss of motor/sensory function.

With the capacity to self-renew and differentiate into various lineages, stem cells represent an important paradigm of cell-based therapy for SCI. Currently the various sources of engrafted cells mainly include neural stem cells, olfactory ensheathing cells, induced pluripo-
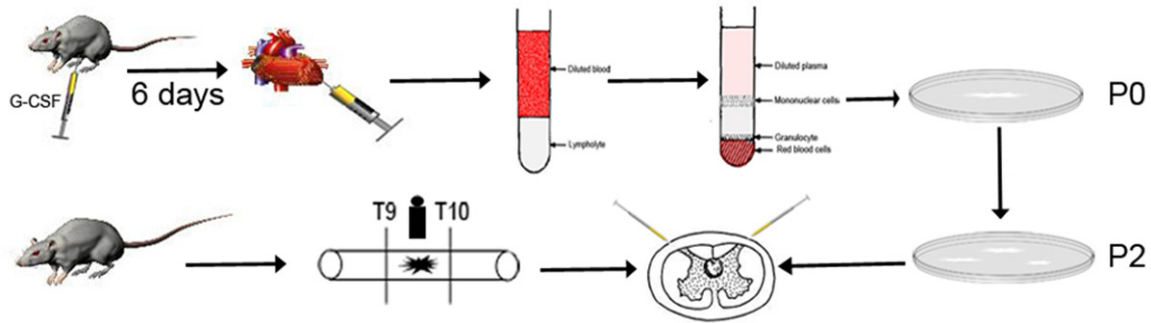
Figure 1. Process of isolation, culture transplantation of PBMSCs. SD rats weighing 80-120 g were subcutaneously injected with G-CSF for 6 d. About 6 ml of peripheral blood was harvested from the left ventricle after anesthetization. Then the sample was diluted with a same volume of PBS and immediately overlaid on rat Ficoll lymphocyte separation liquid. After centrifugation, the cells were cultured until at 80%-90% confluence and then subcultured. Adult rats underwent a contusion of spinal cord for model control after dorsal laminectomy. Following dorsal laminectomy at T9-T10 level, spinal cord was contused with a new type spinal cord impactor. Thirty minutes after SCI, 10 μl of PBS and PBMSC suspension (2×10⁴ cells/μl) were respectively injected into each rat in both the PBS and PBMSCT groups at 2 μl/min and the injection sites were adjacent rostral and caudal spinal cord at a distance of 0.05 mm from the lesion.

tent stem cells, Schwann cells and mesenchymal stem cells (MSCs) [3-9]. Of those, Bone marrow-derived mesenchymal stem cells (BMMSCs) and Umbilical cord-derived mesenchymal stem cells (UCMSCs) possess convenient collection, low immunogenicity and easy expansion *ex vivo*. Thus, BMMSCs and UCMSCs have generated great interest among researchers for SCI therapy [3, 4, 10]. Nevertheless, there is a significant decline in the number, and proliferative and differential capacity of BMMSCs with ages [11]. In addition, the collection of bone marrow aspirate may cause infection and pain. As for UCMSCs, the ethical dispute and inconvenience for autograft have limited their widespread application to some extent. Recently, some studies have documented that peripheral blood-derived mesenchymal stem cells (PBMSCs) own biological characteristics which are similar to that of BMMSCs and UCMSCs, and also possess much more effective cost, less trauma and no anesthesia [12-16]. While, when originating from different sources, capacities of generation and differentiation of MSCs may differ [17]. It is also reported that PBMSCs, isolated from rabbit peripheral blood after mobilization with Granulocyte Colony-Stimulating Factor (G-CSF) and AMD3100 owes stronger differential capacities into adipocytes and chondroblasts than BMMSCs *in vitro* [18]. Many researchers have applied PBMSCs for dental implants, critical-sized calvarial bone defects, middle cerebral artery occlusion and traumatic brain injury *etc.* [19-23] and we have

also transplanted PBMSCs for osteonecrosis of the femoral head in rabbits and SCI in rats [24, 25], which all received good outcomes. In the present research, we engrafted PBMSCs into injury sites after SCI and study the survival, differentiation, protection and immunoregulation of the engrafted cells. It may provide useful experimental evidence of PBMSC-based therapy on SCI for further application.

Materials and methods

Animals

SD rats in a specific pathogen free (SPF) grade were purchased regardless of sex from the Animal Center of Third Military Medical University (production license: SCXK Yu 2012-0005). The animal studies were performed in accordance with the recommendations of the Weatherall report after receiving approval of the Institutional Animal Care and Use Committee (IACUC) in Zunyi Medical College.

Isolation, culture, identification and labeling of PBMSCs

Isolation and culture of PBMSCs were performed according to our previous method as it was illustrated in **Figure 1** [24]. Briefly, SD rats weighing 80-120 g (n = 5) were subcutaneously injected with G-CSF (100 μg/kg/d) for 6 d. After the rat was anesthetized with 10% chloral hydrate (0.35 ml/100 g), 5-8 ml of peripheral blood was harvested from the left ventricle.

Then the sample was diluted with a same volume phosphate buffer saline (PBS) and immediately overlaid on rat Ficoll lymphocyte separation liquid (1.083 g/L; Chuanye Biochemicals, Tianjin, China). After centrifugation at 400×g for 20 min, the intermediate layer was collected and rinsed twice with appropriate PBS. After centrifugation at 250×g for 10 min, the cells were cultured in 5 ml of α-Eagle's Minimum Essential Medium (α-MEM, Gibco, New York, USA), supplemented with 15% fetal bovine serum (FBS, Gibco, New York, USA), 100 U/ml penicillin, 100 µg/ml streptomycin and 2 mmol/L glutamine (Hyclone, Logan, USA). Half of the medium was replaced after 4 d and the full medium was replaced every 3 d. The cells were subcultured at 80%-90% confluence. Passage 2 (P2) cells were analyzed by flow cytometry. Briefly, P2 were collected, treated with 0.125% trypsin (Gibco, New York, USA), suspended by 0.1% BSA and adjusted to 2× 10^6/ml. Afterwards, 100 µl of the suspension was placed into flow tubes, Alexa Fluor® 488 anti-rat CD29, Alexa Fluor® 488 anti-rat CD90, Alexa Fluor® 488 anti-rat CD45, Alexa Fluor® 488 anti-rat CD44, Alexa Fluor® 488 anti-rat CD34 and Alexa Fluor® 488 anti-rat G-CSFR (eBioscience, San Diego, USA) were added into each tube respectively. The samples were detected and analyzed using the FACS Calibur (BD, Franklin L, USA) and the analytic software was Cell Quest. Additionally, 0.125% trypsin-treated P2 cells ($4×10^6$) were labelled with PKH26 (PKH26 Fluorescent Cell Linker Kits, Sigma, USA) and then cultured till P3 for transplantation. Mesoderm multi-lineage differentiation capacities were analyzed according to our previous research [24].

Animal model of SCI and PBMSCs transplantation

Adult SD rats (weighting 200-250 g) were randomly selected according to coin tossing and divided into 4 groups: sham operation group (n = 13), model group (n = 15), PBS control group (n = 15) and PBMSCs transplantation (PBMSCT) group (n = 24, nine for immunofluorescence). Rats in the sham operation group only underwent dorsal laminectomy for blank control. Model group, underwent a contusion of spinal cord for model control after dorsal laminectomy. Rats were anesthetized with 10% chloral hydrate. Following dorsal laminectomy at T9-T10 level, spinal cord was contused with a new type

spinal cord impactor (Chinese patent number: ZL201420557908.8) as previously described [24]. Thirty minutes after SCI, 10 µl of PBS and PBMSC suspension ($2×10^4$ cells/µl) with PBS were respectively injected into each rat in both the PBS and PBMSCT groups at 2 µl/min and the injection sites were adjacent rostral and caudal spinal cord at a distance of 0.05 mm from the lesion (**Figure 1**). The rats for immunofluorescence were injected with PKH26-labelled PBMSCs. Then, muscle and skin layers were sutured. The bladder was emptied by manual abdominal pressure every 8 h until the bladder function recovered. Penicillin was intraperitoneally injected at $16×10^4$ IU/d for 5 d for infection prevention.

Behavioral analysis

Functional recovery of hindlimb motor was evaluated according to the Basso, Beattie, and Bresnahan (BBB) locomotor rating scale [26]. Briefly, preoperative and postoperative testing session were conducted for 4 min when rats in each group walked continuously in the open field using the BBB locomotor rating scale. The standardized 21 point scale is mainly based on hindlimb movement and locomotor efficiency, 0 represents complete paralysis and 21 normal. Tilt table test was operated for detection of the degree of paralysis according to the reported method [27]. Briefly, rats in each group were placed onto a rubber-covered movable board, and the longitudinal axis of the tested rat was perpendicular to that of the inclined plate. Then the plate end which rat heads were directed towards was raised until the animal finally slid down. The maximum angle at which the rats could stay for at least 5 s was then recorded. Both the person producing the lesion and the tester assessing outcomes were masked to all group assignment. Additionally, the time of bladder functional recovery was recorded any time.

Histopathology analysis and Luxol Fast Blue staining

Histopathology and Luxol Fast Blue (LFB) were performed according to the reported methods to see the protection of PBMSCs on myelin sheathes and neurons with the previous methods [28]. Briefly, after anesthetized with 10% chloral hydrate, three rats in each group were transcardially perfused with 4% paraformalde-

hyde (PFA) at the corresponding time. Then a 6 mm-long spinal cord including the lesion was collected. After fixed with 4% PFA for 24 h, the tissue specimen underwent conventional dehydration and was embedded in paraffin wax and cut at 4 µm. Some were used for H&E staining, some for Luxol Fast Blue (LFB) staining, the left for immunohistochemistry. For LFB staining, after deparaffinization and clearance with 100% and 95% ethanol, staining with 60% LFB solution, rinse with 95% ethanol, 0.05% lithium chloride solution and 70% ethanol and distilled water, slides were sealed with Polyvinylpyrrolidone Mounting Medium (PVP, Beyotime, Shanghai, China).

Immunohistochemical staining

Immunohistochemical staining was performed according to instructions of manufacturer (GTVision™⁺ Detection system kit, Gene Tech, Shanghai, China). Briefly, paraffin sections were blocked with 10% goat serum for 30 min at room temperature. Primary antibodies were then respectively dropped onto the fixed sections overnight at 4°C. For primary antibodies, we used Anti-glial fibrillary acidic protein (GFAP) polyclonal antibody (1:300; Abnova, Taiwan, China), Anti-myelin basic protein (MBP) antibody (1:200; Abcam, Massachusetts, USA), Anti- neurofilament protein-200 (NF-200) antibody (1:100; Abcam, Massachusetts, USA) and Anti-glial fibrillary acidic protein (MAP-2) antibody (1:200; Abcam, Massachusetts, USA), Anti-IL6 antibody (1:100, Sigma), Anti-IL17 antibody (1:100, Sigma) and Anti-TGF-β antibody (1:100, Sigma) and PBS was used as negative control. After the sections were washed with PBS the following day, HRP-conjugated secondary antibodies (Solution A of GTVision™⁺ Detection system kit) were added and then the sections were incubated for 30 min at room temperature. Thereafter, the sections were washed with PBS 3 times, covered with DAB working solution, counterstained with hematoxylin, dehydrated through graded alcohols, cleared with xylene and sealed with Polyvinylpyrrolidone Mounting Medium (Beyotime, Shanghai, China). Integral optical density (IOD) of the positive staining was then measured.

Immunofluorescence staining

After perfused with 4% PFA, dehydrated through graded sucrose and embedded in OCT, the injured spinal cord specimen (n = 3 at each time point) was cut at 8 µm by freezing microtome (CM 1850, Leica, Germany) for immunofluorescence staining. The collected frozen sections were dried at room temperature for 10 min and washed 3 times. After blocked with 10% goat serum and dropped with primary antibodies overnight according to the steps mentioned above, the sections were covered with Goat anti-rabbit/mouse IgG-FITC (Jackson, West Grove, PA) and incubated for 30 min at 37°C. For primary antibodies, we used Anti-GFAP polyclonal antibody (1:300; Abnova, Taiwan, China), Anti-MBP antibody (1:200; Abcam, Massachusetts, USA), and Anti-Neuronal specific neucleoprotein (NeuN) antibody (1:300; Abcam, Massachusetts, USA). Subsequently, these sections were washed with PBS, stained with DAPI, sealed with Antifade Polyvinylpyrrolidone Mounting Medium (Beyotime, Shanghai, China) for analysis under a fluorescence microscope (DMIR, Leica, Solms, GER).

Flow cytometric analysis

On days 14, 28, and 56 after transplantation we investigated the frequency of CD4+IL17+Th17/CD4+CD25+Foxp3+ regulatory T (Treg) cells according to the previous reports [29]. Individual cell suspensions from the PBMNCs and spleen were isolated and 2×10^5 cells in each tube were resuspended with RPMI 1640 medium modified (Hyclone; Logan, Utah, USA) supplemented with 10% fetal bovine serum (FBS; Gibco, New York, N.Y., USA) and pre-cultured with BFA/Monensin Mixture (250×, 0.75 mg/ml and 0.35 mg/ml, Multi Sciences), PMA/Ionomycin Mixture (250×, 12.5 mg/ml and 0.25 mg/ml, Multi Sciences) for 4 h before intracellular staining. After resuspended by Flow cytometry Staining buffer, Th17 cells were stained with Anti-Rat CD4 FITC (eBioscience, San Diego, Calif., USA), incubated for 1 h at 4°C avoiding light and then pretreated with Fix & PERM Kit (Multi Sciences). Anti-Mouse/Rat IL-17A PE (eBioscience) were then added and the cells were incubated in the dark for 1 h at room temperature. For CD4+CD25+Foxp3+Treg cells staining, Anti-Rat CD4 FITC and Anti-Rat CD25 PE (eBioscience) were added into the individual cell suspensions from the PBMNCs and spleen and those cells were incubated for 1 h at 4°C avoiding light. One ml of Foxp3 Fixtion/Permeabilization working solution were then added to each tube for incuba-
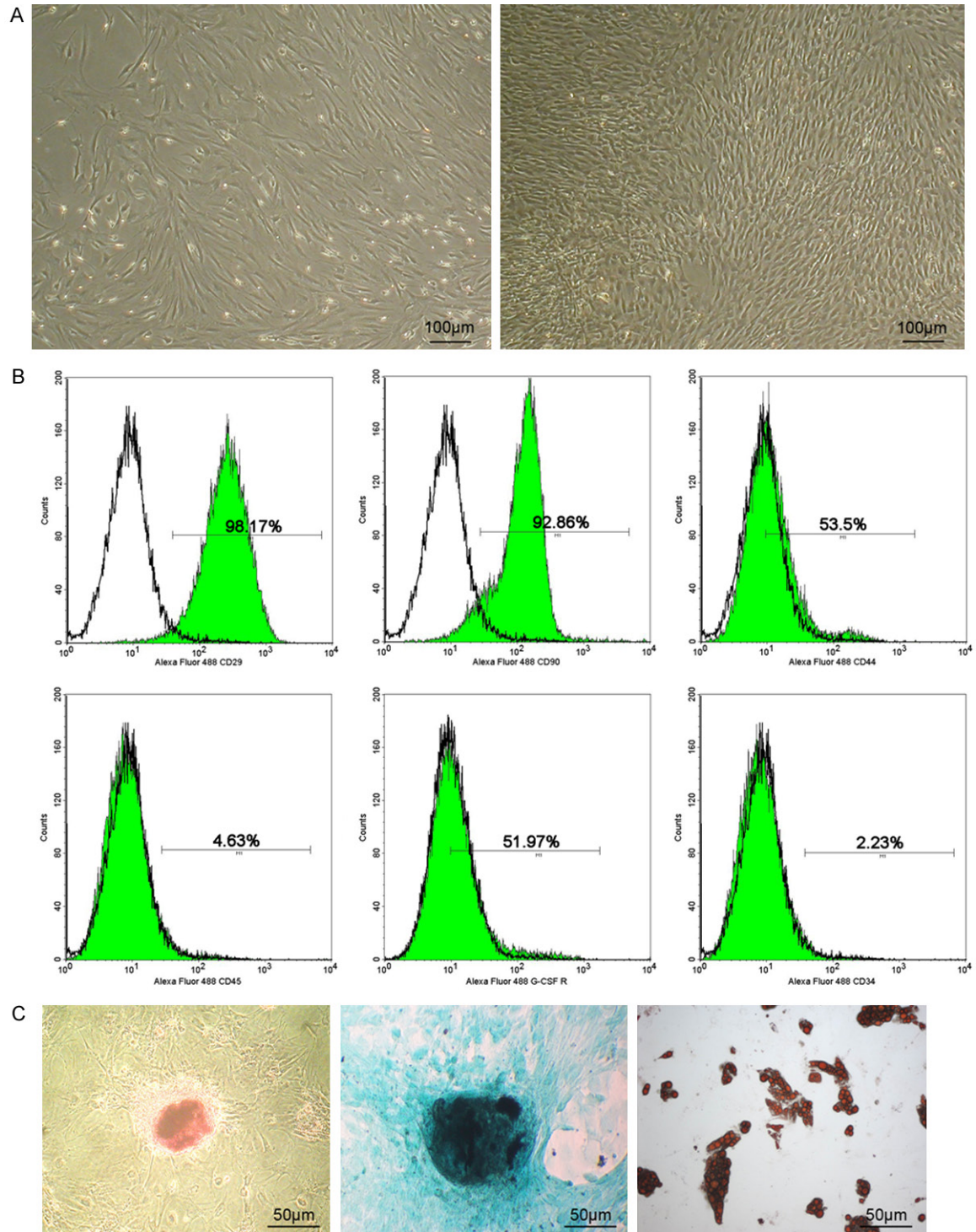
Figure 2. Morphology and identification of PBMSCs. A: Primary culturing PBMSCs owned a uniform and long-spindle shape and arranged radially at 16th day under light microscope and PBMSCs after subculture still kept that shape; B: P2 cells could express positively CD90, CD29, CD44, G-CSFR, but negatively CD34 and CD45. C: Osteogenesis, chondrogenesis, adipogenesis-committed differentiation of PBMSCs respectively by alizarin red, alcian blue and oil red.

tion in the dark at room temperature for 1 h. Data analysis were performed with a flow cytometer (FACS Calibur; BD) using Cell Quest analytic software.

Cytokine assay

Serum was collected from rats 14 d, 28 d and 56 d postinjury. Cytokines TGF-β (Rat TGF-beta1 Platinum ELISA, eBioscience), IL-6 (Rat IL-6 Platinum ELISA, eBioscience) and IL-17a (Rat IL-17A Platinum ELISA, eBioscience) were measured using commercial ELISA kit according to the manufacturer's instructions.

Reverse transcription-polymerase chain reaction (RT-PCR)

RT-PCR was performed according to the previous study [25]. Total RNA was extracted from the freshly isolated spinal cords of every group at the end of the experiment (day 56) using Trizol (Invitrogen, Carlsbad, USA) reagent according to the manufacturer's protocol, a reverse transcription reaction was performed using PrimeScript® RT Reagent Kit (TaKaRa, No.RR037A, Dalian, China); a reverse transcription reaction was performed by a PrimeScript® RT Reagent Kit (TaKaRa, No.RR037A, Dalian, China) in a 10-μl reaction volume and the reaction conditions was set to 37°C for 15 min and then 85°C for 5 s; the reaction system of fluorescent quantitative PCR was carried out with a SYBR® Premix Ex TaqTM Kit (TaKaRa, No.RR-420A, Dalian, China). Primer sequences were listed as follows and β-actin gene was used as an internal control. RORγT: 5'-AGACACCAC-CGAACATCTCG-3' (forward), 5'-AGGAGTAGGC-CACATTGCAC-3' (reverse); FoxP3: 5'-AGCTTGT-TTGCTGTGCGGAG-3' (forward), 5'-GTGGCATAG-GTGAAAGGGGG-3' (reverse); IL-17a: 5'-CAAACG-CCGAGGCCAATAAC-3' (forward), 5'-AGAGTCC-AGGGTGAAGTGGA-3' (reverse); IL-6: 5'-TTCACA-GAGGATACCACCCACA-3' (forward), 5'-AATCAG-AATTGCCATTGCACAA-3' (reverse); IL-22: 5'-AGT-CACCTCAGCCCCTGTCAC-3' (forward), 5'-CCC-GATCGCTTTAATCTCTCC-3' (reverse); IL-23a: 5'-GGTGATGGTTGTGATCCCCA-3' (forward), 5'-AT-GTCCGAGTCCAGCAGGTG-3' (reverse); IL-21: 5'-GCACGAAGCTTTTGCCTGTT-3' (forward), 5'-GGC-ATTTAGCCATGTGCCTC-3' (reverse); IL-10: 5'-GA-AAAATTGAACCACCCGGCA-3' (forward), 5'-TTC-CAAGGAGTTGCTCCCGT-3' (reverse); TGF-β: 5'-CCGCAACAACGCAATCTATG-3' (forward), 5'-AGC-CCTGTATTCCGTCTCCTT-3' (reverse).

Statistical analysis

Experiment data were presented as mean ± standard error (SEM). Statistical analyses were conducted using the SPSS 13.0 software package. One-way or two-way ANOVA was performed for comparison between groups. Statistical significance was set at $P < 0.05$.

Result

Morpholog and identification of PBMSCs

A few cultured cells could grow adherently 48 h after primary culture, obvious colony formed 9 d later, cell confluence got 70%-80% 16 d later and those cells could cover the bottom of the bottle 20 d later (**Figure 2A**). Passaged cells owned a uniform and long-spindle shape and arranged radially (**Figure 2A**). Flow cytometry showed positive expression of CD90, CD29, CD44, and G-CSFR, but negative expression of CD45 or CD34 (**Figure 2B**). Also, those cells owned multi-lineage differentiation potency into adipocytes, chondrocytes and osteocytes (**Figure 2C**).
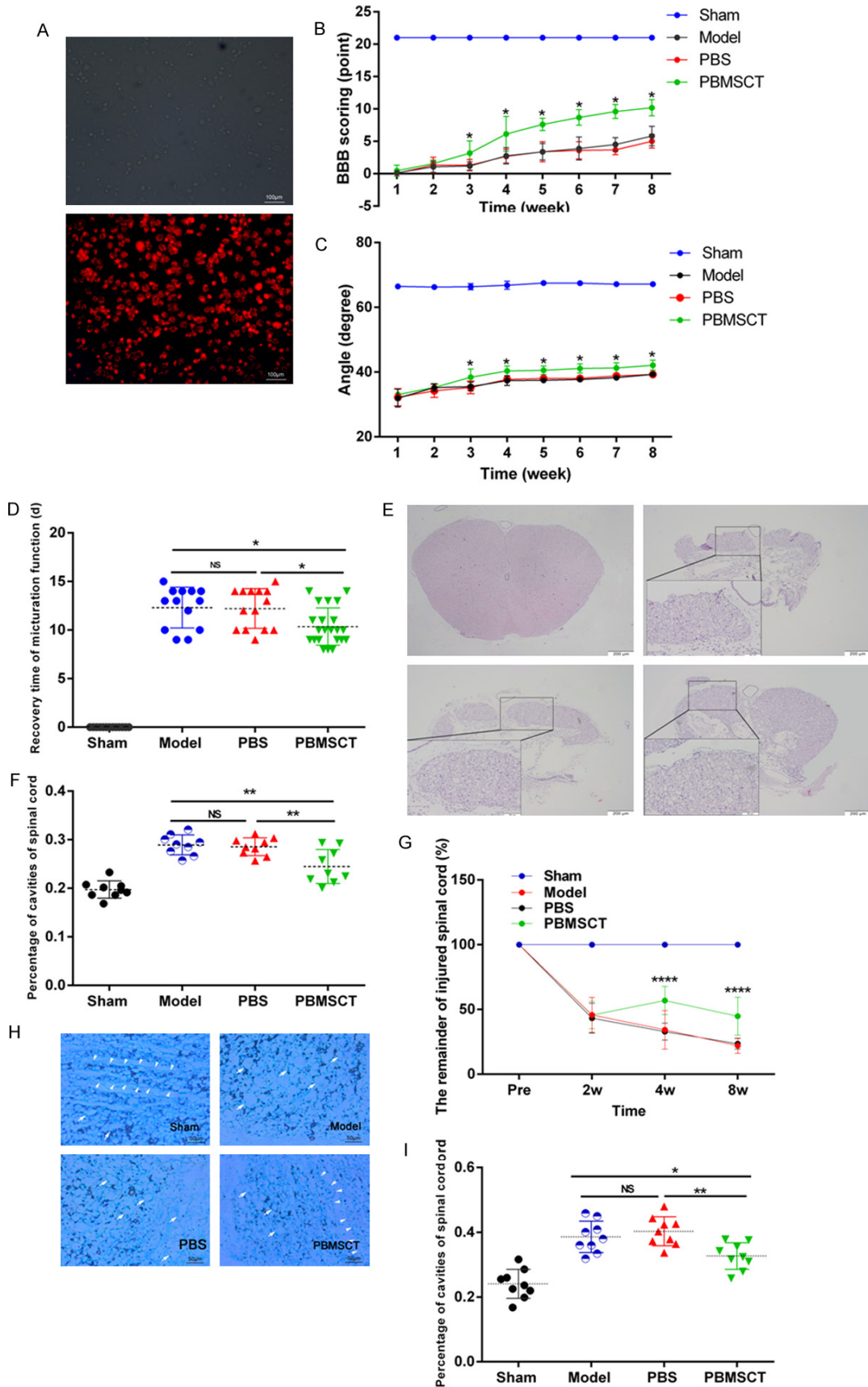
Functional recovery

After labelled with PKH26, those cells, with an intact cell membrane, showed a well-delineated red fluorescence. After calculation, we got that the labeling rate > 99% (**Figure 3A**). BBB locomotor rating scales of all animals were 21 points 1 d before operation. BBB scoring of the rats in the sham operation group were also 21 points throughout the period of the experiment. On the day of operation, all models in the other 3 groups showed complete paralysis. Until 3rd week after operation, PBMSC-injected rats showed a significantly higher BBB rating scale than the PBS-injected and nothing-injected rats ($P < 0.05$). There was no significant difference observed between PBS-injected and nothing-injected rats after SCI (**Figure 3B**). Similar to the BBB data, tilt plate test signified a lager angle after PBMSCT (**Figure 3C**). In addition, rats after PBMSCT treatment owned a quicker micturation recovery ($P < 0.05$; **Figure 3D**).

PBMSCT could promote the restoration of histopathological alteration

H&E results implied that the margins between gray and white matter was distinct after sham operation 56 d postinjury. Significant gliosis and abundant cavities occurred in the PBS and model group. By contrast, less gliosis and cavities could be observed after PBMSCT ($P < 0.05$;

Figure 3. Labelling rate of PBMSCs, functional recovery after PBMSCT. A: PBMSCs after BrdU labelling *in vitro* under phase contrast microscope and under fluorescent microscope). B, C: BBB scoring and tilt table test of rats in each group. There were a lager angle and higher BBB scoring after PBMSCT (n = 22 as two died from apastia 7 d after surgery) than both in the Model group (n = 13 as one died 1 d after surgery and another died 5 d later) and PBS group (n = 14 as one died 4 d after surgery). D: Rats after PBMSCT showed a quicker micturition recovery time. E-G: Clear boundary still existed between gray and white matter, neat-arranged nerve fiber bundles, regular neuronal morphology in the sham operation group; boundary between gray and white matter disappeared and severe disintegration of neuron-like cells, cavity formation and gliosis were observed in both the model and PBS groups after SCI. While there was less cavities and more tissue preservation in the PBMSCT group at 8 w (n = 3). H, I: LFB results manifested that PBMSC-treated rats presented a relatively lower cavities and discontinuous myelin sheath (n = 3). Data represented Mean ± SEM, $^*P < 0.05$, $^{**}P < 0.01$, $^{****}P < 0.00001$, NS: no significance.

Figure 3E, **3F**). Additionally, tissue could be preserved more (**Figure 3G**). Meanwhile, LFB staining manifested a regular arrangement of myelin sheath in rats only undergoing sham operation, while presented an irregular or completely disappear myelin sheath, flooded with abundant cavities after SCI. In contrast, PBMSC-treated rats presented a relatively lower cavities and discontinuous myelin sheath ($P < 0.05$; **Figure 3H**, **3I**). These result inferred PBMSCT could promote the injury recovery, protect the neurons and myelin sheathes in the injured lesion.

Protection-relevant gene expression analysis by immunohistochemistry and immunofluorescence

GFAP, MBP, NF-200 and MAP-2 could express to some extend in all groups. At 2 w after SCI, GFAP, MBP, NF-200 and MAP-2 expression in the PBMSCT group were respectively higher than that in the model and PBS groups ($P < 0.01$); at 4 and 8 w, GFAP expression in the model and PBS groups increased abruptly and were higher than that in the PBMSCT group ($P < 0.01$) and glial scars formed significantly, and MBP, NF-200 and MAP-2 expression still kept the same tendency as that at 2 w ($P < 0.01$, **Figure 4A**, **4B**). Immunofluorescence staining revealed engrafted PKH26+PBMSCs (the red color) could survived at the injury site for at least 8 w. However, there were little PKH26+GFAP+FITC astrocytes, PHK26+MBP+FITC oligodendrocytes, PKH26+NeuN+FITC neurons could be observed, which indicated the PBMSCT-relevant therapy took effect not through the differentiation of PBMSCs into CNS cells (**Figure 4C**).

Effect of PBMSCs on Th17/Treg cell balance

It was reported that suppression of Th17 lymphocyte differentiation could promote locomotor recovery in mice after SCI, which implied the

impairment of Th17 lymphocytes in SCI [30]. CD4+T lymphocytes, could be differentiated from CD4+T cells in the presence of TGF-β and possessed a crucial role in controlling immune responses to self-antigens and preventing autoimmune diseases and [31]. The similar regulatory pathway (STAT3 signaling), makes it paramount to study Th17/Treg balance. The data implied that CD4+IL17+Th17 cells presented a high population in spleen and PBMNCs in the model and PBS group while a relatively low number after PBMSCT treatment 14 d postinjury (**Figure 5A-C**). Meanwhile there was an increased percentage of CD4+CD25+Foxp3+Treg cells after PBMSCT, higher notably than that without PBMSCT (**Figure 5D-F**). These results suggested that PBMSCT could prevent the differentiation of Th17 cells and promote the differentiation of Treg cells after SCI.

Analysis IL-6, IL-17a, and TGF-beta expression in the injured lesion

To further certify the immunoregulation function of PBMSCs on injured lesion, we analyzed IL-6, IL-17a and TGF-β expression by immunohistochemistry. As presented in the **Figure 6**, IL-6 and IL-17a expression were suppressed while TGF-β expression were promoted in the injured lesion after PBMSCT.

Analysis cytokines IL-6, IL-17a and TGF-β levels in SCI rats

To study whether PBMSCs impacted on repair by immunoregulary function through blood circulation, we analyzed TGF-β, IL-6 and IL-17a level changes. As demonstrated in the **Figure 7A**, IL-6 and IL-17a were markedly suppressed ($P < 0.05$) while the production of TGF-β showed a distinct increase ($P < 0.05$) in the PBMSC-treated serum by Elisa from day 14 on. The data implied that PBMSCs might immunoregulate protein expression of Th17/Treg cell in SCI rats.
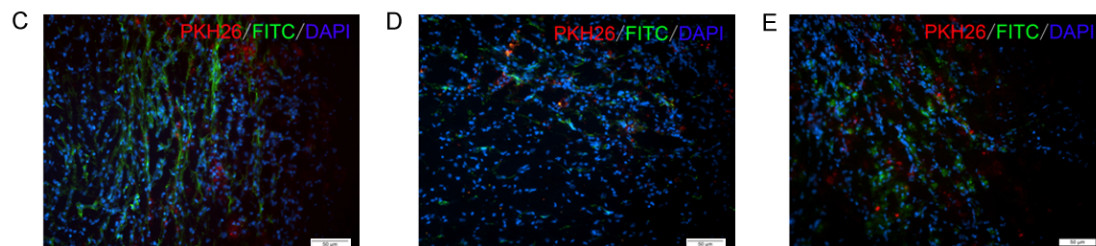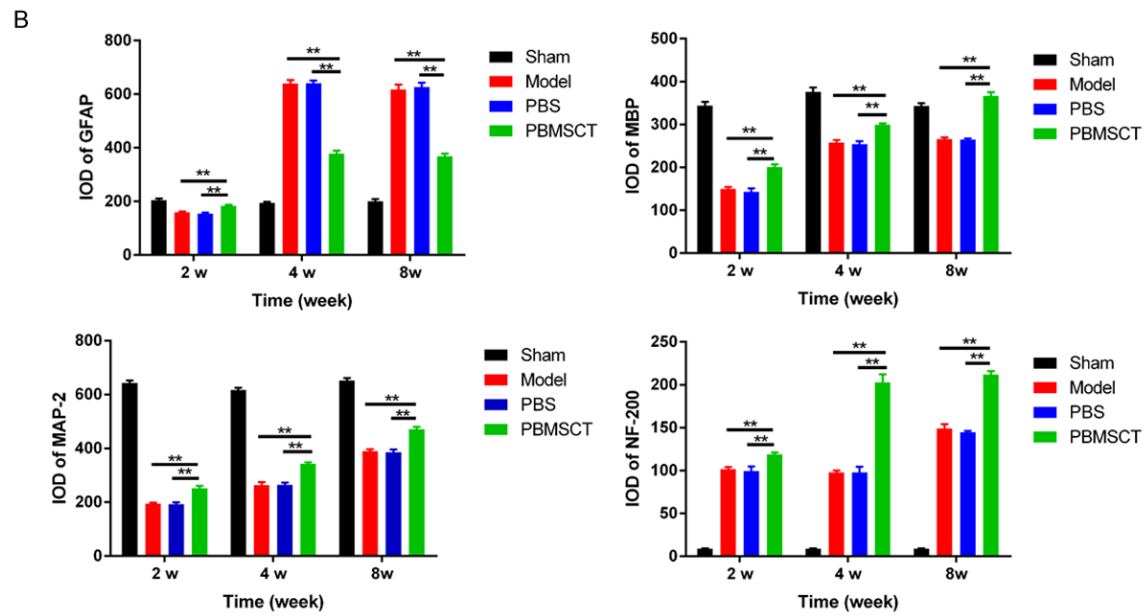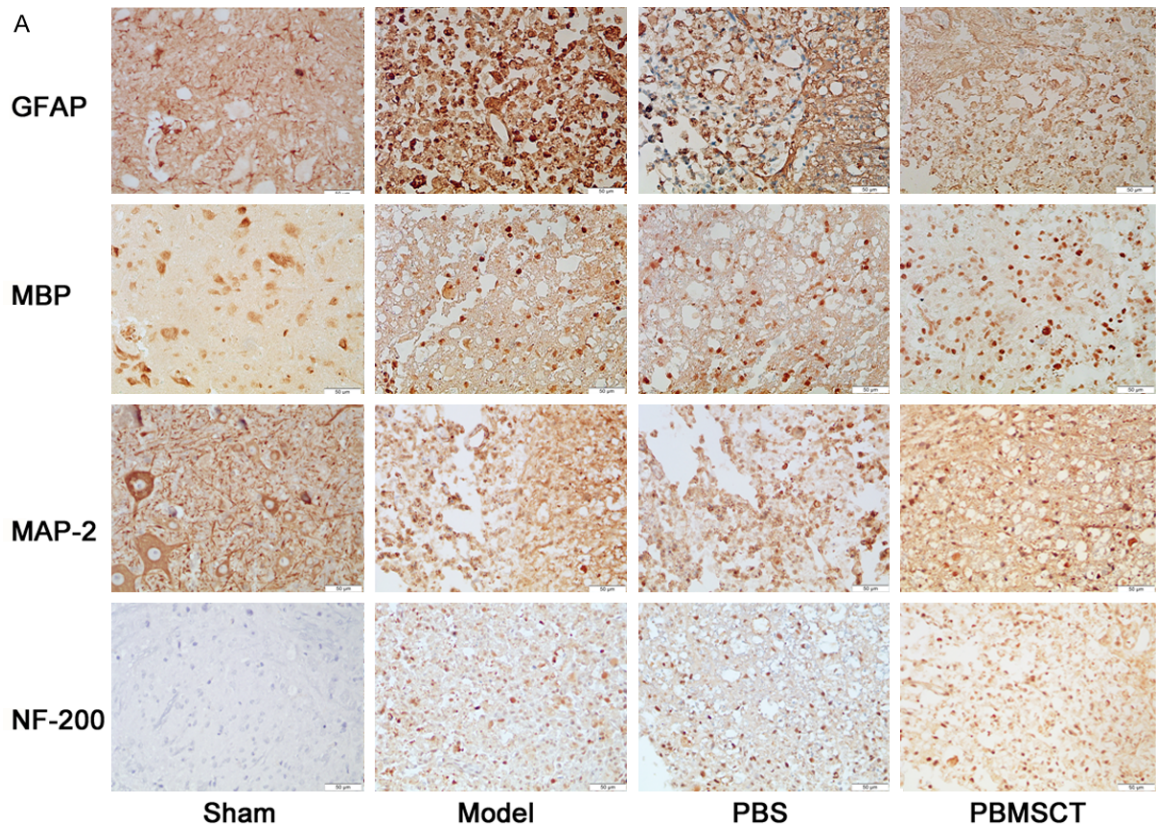
Figure 4. Immunohistochemistry and immunofluorescence analysis of the protective-relative proteins after PBM-SCT. A, B: There was a lower IOD at 4 w and 8 w and there was no glial scar observed and a lower GFAP expression after PBMSCT (n = 3 in each group at each time point); higher expression of MAP-2, MBP and NF-200 could be observed obviously after PBMSCT corresponding time point. C-E: There were little implanted PKH26-labelled PBM-SCs could co-express GFAP, MBP and NeuN. The number of survival PKH26+ cells reached as long as 8 w. Data represented Mean ± SEM, $^{**}P$ < 0.01.

Expression analysis of genes relative to Th17/ Treg balance

RT-PCR data indicated that a lower expression of Th17-relevant genes including RORγT, IL-6 and resulting in the secretion of IL-23a and IL-22; meanwhile and the expression of Treg-relevant genes including FoxP3 and TGF-β were improved, resulting in the overexpression of IL-10 and TGF-β (P < 0.05, **Figure 7B**). The data indicated that PBMSCs could change the Th17/ Treg cell balance though factor secretion change.

Discussion

The differential potency into neural-like and glial-like cells and self-renew capacity makes MSCs suitable for therapy of CNS diseases, such as SCI [32, 33]. To data, numerous studies have reported MSC transplantation for SCI improves tremendously the recovery of locomotor function after SCI [3, 4, 10, 34-36]. Though PBMSCs were similar to BMMSCs in many characteristics, the differentiation of two seed cells into adipocytes had significant difference. There are little reports about PBMSCT for SCI therapy until now. In our previous studies, PBMSCs could differentiate into neurons under induced medium *in vitro*, which makes PBMSCT possible for SCI treatment [37]. Here, the data of tilt table test, BBB locomotor rating scales and bladder functional recovery suggested that rats after PBMSC therapy owned better motor performance. Additionally, there was not any abnormal behavior emerging in the whole progress. H&E as well as LFB staining revealed there were less necrotic cavities formed, more tissue preserved and no glial scar occurred in the species from PBMSC-injected rats at 8 w. It preliminarily confirmed PBMSCT was a useful strategy to enhance functional recovery, inhibit glial scar formation and protect myelin sheath.

How did PBMSCs take effects? Nowadays, the mechanisms of MSC therapy mainly focuses on the differentiation into the lost CNS cells, that is replacement therapy, and another is immunoregulation. Firstly, replacement therapy means the differentiation into the lost astrocytes, oligodendrocytes and neurons. Therefore, it's necessary to explore the expression of the relevant characteristic proteins such as MBP and NeuN. As a major component of oligodendrocytes and Schwann cells, MBP plays important roles in the velocity of axonal impulse conduction and maintenance of correct structure of myelin [38, 39]. The inhibition of glial scar formation mainly depends upon astrocyte cells, which can express numerous GFAP [40]. It plays an important role in mitosis and astrocyte-neuron interactions as well as cell-cell communication [41, 42]. NF-200 is a maker of axon sprouting and regeneration [43]. MAP-2 mainly exists in the neuronal cell bodies and dendrites and is the maker of dendrite growth and plays an important role in neuronal development and synaptic plasticity [44]. Once the regeneration of neurons occurs, NF-200 and MAP-2 can be overexpressed. Therefore, we explored the relevant-protein expression combining immunohistochemistry with immunofluorescence to study the underlying mechanisms of replacement treatment. It showed GFAP, MBP, NF-200 and MAP-2 expression after PBMSCT were respectively higher 2 w post-injury. As time gone, GFAP decreased while other 3 factors were still a higher tendency. Astrocyte cells at different stage (naïve and mature) play different roles in the pathological and physiological process of SCI [45, 46]. Naïve astrocytes, with active anabolic effects, form the cellular grid framework and induce the regeneration of nerve fibers while mature ones transform structural cells and proliferate forming scars which can block nerve regeneration. We hypothesized that engrafted PBMSCs could differentiate into naïve astrocytes or improve the number of naïve astrocytes and meanwhile inhibit the number of mature ones. Additionally, there were little PKH26+GFAP+FITC astrocytes, PHK26+MBP+FITC oligodendrocytes, PKH26+NeuN+FITC ne-
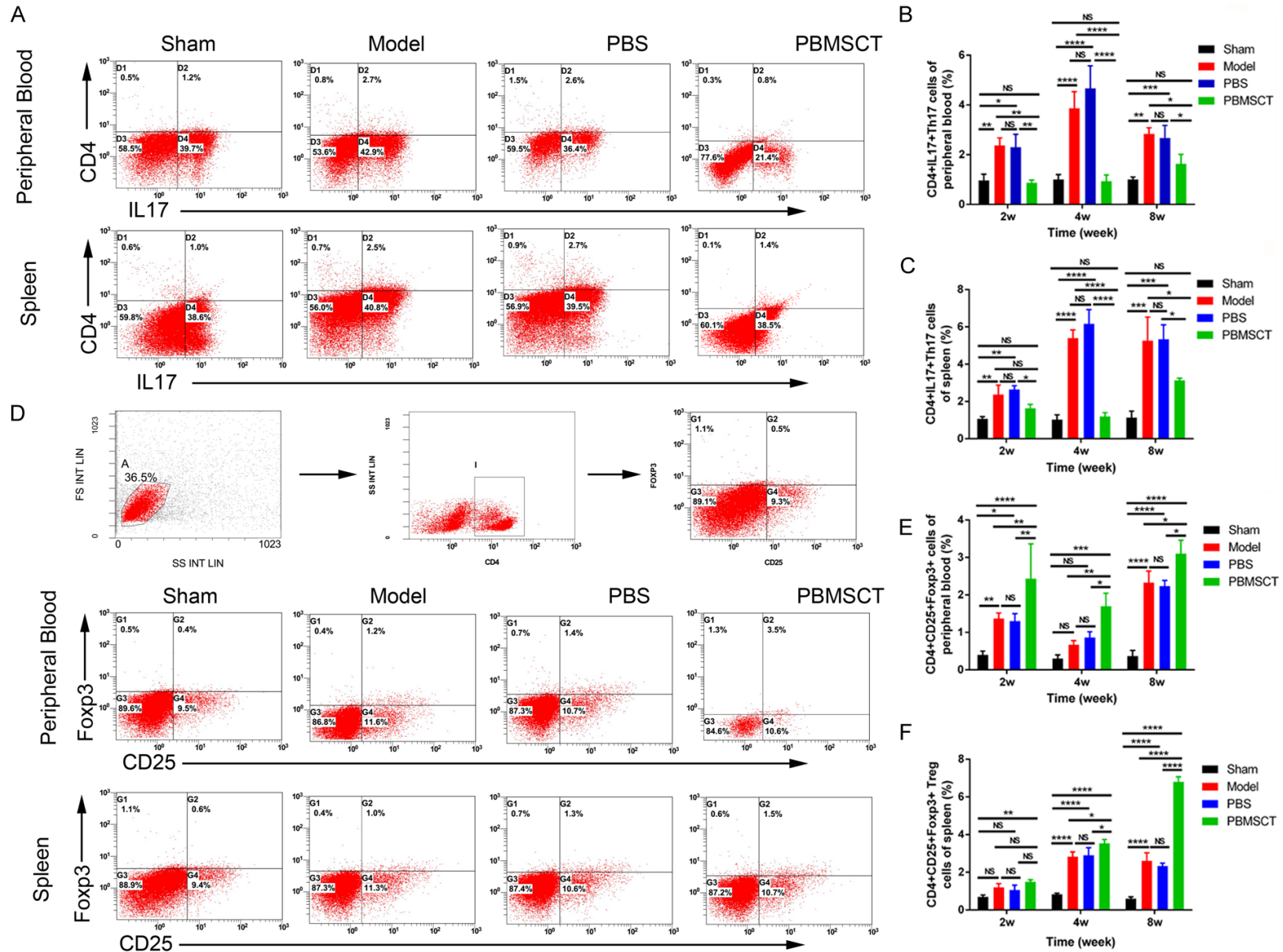
Figure 5. Flow cytometry of Th17/Treg cells in peripheral blood serum and spleen. A-C: CD4+IL17+Th17 cells presented a lower population in PBMNCs and spleen after PBMSCT treatment 14 d post injury. D-F: There were an increased percentage of CD4+CD25+Foxp3+Treg cells after PBMSCT. n = 3 in each group at every time point, data represented Mean ± SEM, *P < 0.05, **P < 0.01, ***P < 0.001, ****P < 0.0001, NS: no significance.
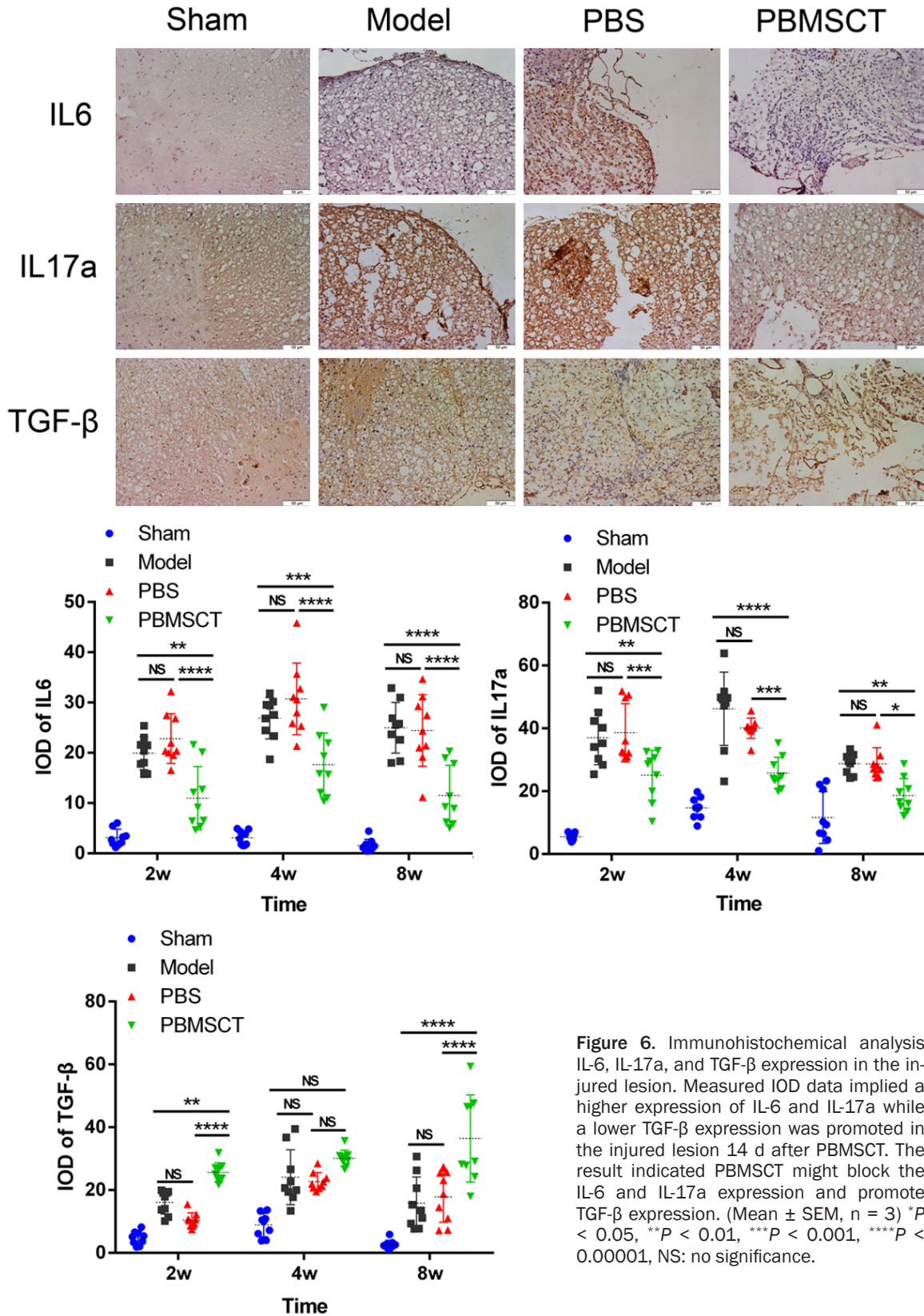
Figure 6. Immunohistochemical analysis IL-6, IL-17a, and TGF-β expression in the injured lesion. Measured IOD data implied a higher expression of IL-6 and IL-17a while a lower TGF-β expression was promoted in the injured lesion 14 d after PBMSCT. The result indicated PBMSCT might block the IL-6 and IL-17a expression and promote TGF-β expression. (Mean ± SEM, n = 3) *P < 0.05, **P < 0.01, ***P < 0.001, ****P < 0.00001, NS: no significance.
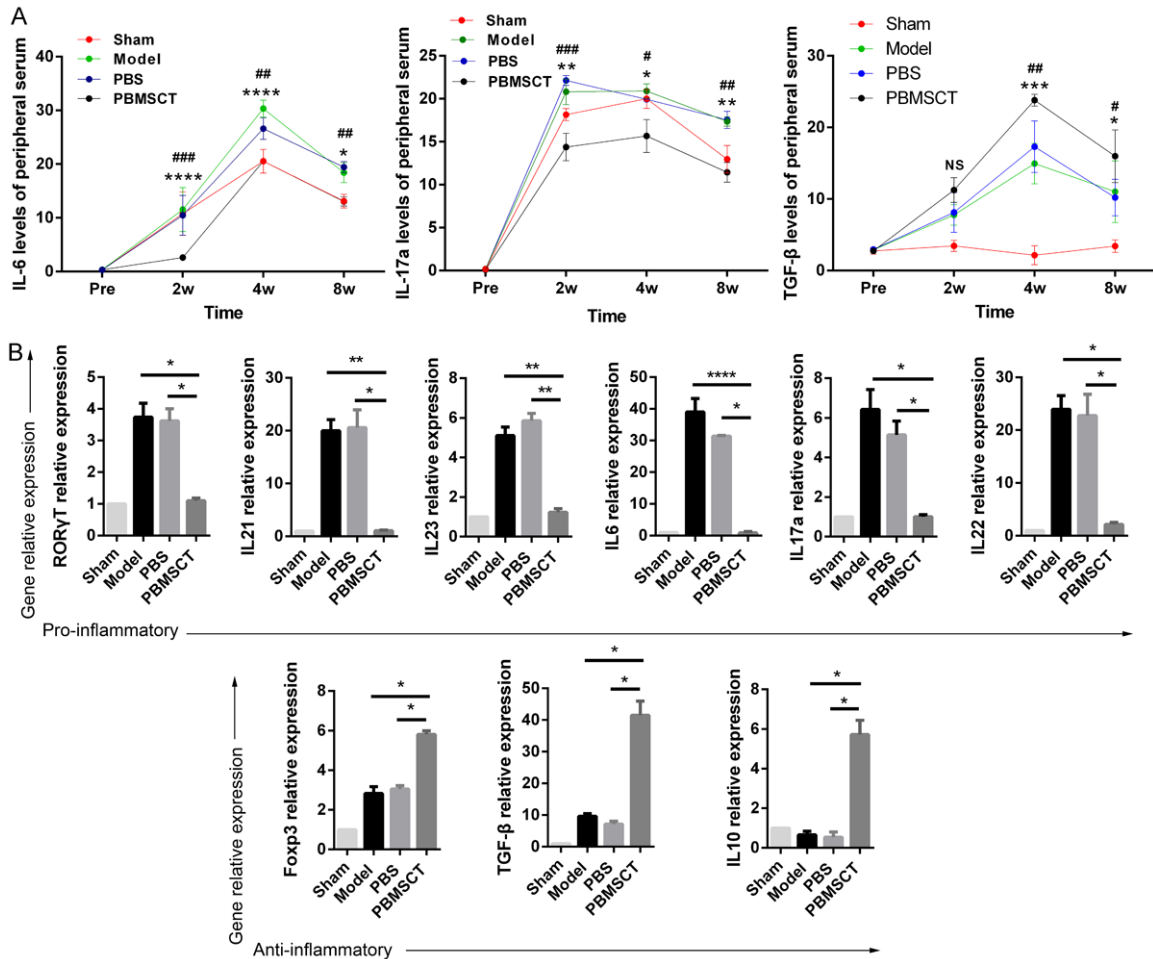
Figure 7. IL-6, IL-17a and TGF-β expression in Peripheral serum and Relative gene expression analysis. A: Unanimous with the result above, IL-6 and IL-17a were markedly suppressed. The production of TGF-β showed a distinct increase in the PBMSC-treated serum by Elisa from day 14 on. The data implied that PBMSCs might immunoregulate protein expression of Th17/Treg cell in SCI rats. n = 3 at each time point in each group. B: Expression of RORγT, IL-6, IL-21, IL-23a, IL-22 were suppressed after PBMSCT and that of FoxP3, IL-10 and TGF-β were promoted to varying extents at 8 w. The data indicated that PBMSCs could change the Th17/Treg cell balance though factor secretion change. n = 4 in each group, data represented Mean ± SEM, $^*P < 0.05$, $^{**}P < 0.01$, $^{***}P < 0.001$, $^{****}P < 0.0001$ model group vs PBMSCT group; $^\#P < 0.05$, $^{\#\#}P < 0.01$, $^{\#\#\#}P < 0.001$ PBS group vs PBMSCT group; NS: no significance.

urons could be observed, which indicated the PBMSCT-relevant therapy took effect not through the differentiation of PBMSCs into CNS cells. Even so, the engrafted PKH26+PBMSCs could survived at the injury site for at least 8 w, obtaining a longer survival time comparing with the previous reports [3, 35, 47, 48].

Another key is inmunoregulatory. It was reported that the number of arginase1+CD206+ macrophage (M2) increased while that of iNOS+ CD16/32+ macrophage (M1) decreased after human BMMSC transplantation for SCI in rats [49]. In our current study on the immunoregulation comparison between BMMSCs and PBMSCs, we found that PBMSCs own a stron-

ger immunoregulation which also inhibited M1 macrophages and promoted M2 macrophages expression (unpublished data). It has been aninamously recognized traditionally that Th17/Treg balance possesses a crucial role in auto-immune diseases. We supposed that PBMSCs could also promote the differentiation of CD4+T lymphocytes into CD4+CD25+Foxp3+Treg ones and meanwhile inhibit into Th17 cells. The flow cytometry data confirmed our reference. In the normal process, Th17/Treg balance is regulated by TGF-β, which can induce gene expression of Foxp3 and RORγT; meanwhile, Foxp3 expression can in turn inhibit RORγT expression [50]. However, this inhibition can be abrogated when IL-6 is present and as a result Th17 differentia-
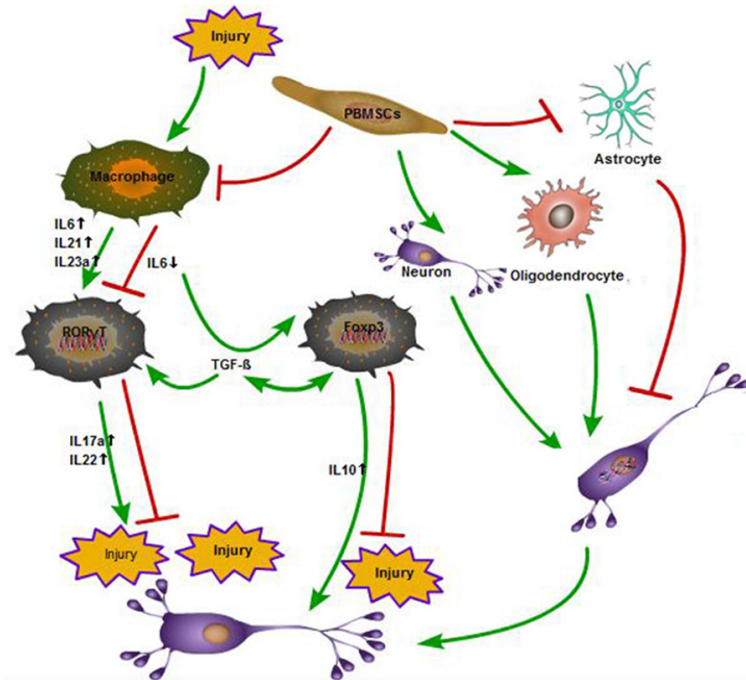
Figure 8. The potential Th17/Treg-relative mechanism of PBMSCs therapy on SCI. Th17/Treg cell balance is mainly regulated by FoxP3 and RORγT; FoxP3 expression can be inhibited by RORγT expression. SCI insulted that M1 macrophage migrated to the lesion and secreted proinflammatory factors such as IL-6 and IL-21 which enabled CD4+T cells to differentiate into CD4+IL17a+Th17 cells which could aggravate the injury and tissue loss in the presence of TGF-β. Then Th17 cells could secret IL-17a, IL-6 and IL-22 *etc.* to promote inflammatory. Meanwhile CD4+T cells are forced into CD+IL17+Th17 cells, as a result the number of Th17 cells are sharply improved and the loss of injured CNS cells. After PBMSCT, IL-6 expression is inhibited obviously, and CD4+T cells are forced into CD4+CD25+FoxP3+Treg cells under the co-influence of TGF-β and FoxP3 could reduce the injury and promote the tissue preservation. Theoretically implanted PBMSCs could not only differentiate the lost oligodendrocytes and Neurons, but also inhibit the overexpression of GFAP. However, there is little differential cells could be observed in this study.

tion can be improved [51]. Then Th17 cells secrete IL-17a and IL-6 to medicate tissue inflammation [52]. Therefore, we analyzed the IL-17a, IL-6 and TGF-β expression at the injury lesion. The results inferred a lower IL-17a and IL-6 while a higher TGF-β level. After the extra analysis of peripheral blood serum and spleen level of IL-6, IL-17a and TGF-β, we could further confirm the effect of PBMSCs on SCI rats. Additionally, in the process of Th17 differentiation, IL-23a and IL-21 might produce marked effects. IL-23a serves as a survival signal for Th17 cells and IL-21, similar to IL-6, may be an additional signal for full function of Th17 cells [51, 53]. When IL-6 is absent, CD4+T cells can differentiate into Treg cells and express IL-10 and TGF-β for anti-inflammatory. PCR data demonstrated the coincidental results of those

relative genes. The relative mechanism could be included as **Figure 8**. What's more, blockade of IL-6 may be an effective therapy on SCI.

Conclusion

PBMSCT-relevant therapy took effect not through the differentiation of PBMSCs into CNS cells, but through regulating Th17/Treg-relevant genes expression, inhibiting Th17-relevant gene expression and meanwhile promoting Treg-relevant gene expression, and eventually resulted in promotion of the functional recovery of SCI rats.

Acknowledgements

Disclosure of conflict of interest

None.

Address correspondence to: Dr. Tao Zhang, Key Laboratory of Cell Engineering of Guizhou Province, Affiliated Hospital of Zunyi Medical College, 149 Dalian Rd., Zunyi 563000, Guizhou, China. Tel: 0086-851-28608806; E-mail: oceanzt@163.com; Dr. Qiang Fu, Sichuan Academy of Medical Sciences and Sichuan Provincial People's Hospital, School of Medicine, University of Electronic Science and Technology of China, 32 West Second Section, First Ring Road, Chengdu 610072, Sichuan province, China. E-mail: johnredfu@163.com

References

[1] Bareyre FM. Neuronal repair and replacement in spinal cord injury. J Neurol Sci 2008; 265: 63-72.

[2] Suberviola B, Gonzalez-Castro A, Llorca J, Ortiz-Melon F and Minambres E. Early complica-

tions of high-dose methylprednisolone in acute spinal cord injury patients. Injury 2008; 39: 748-752.

[3] Park SI, Lim JY, Jeong CH, Kim SM, Jun JA, Jeun SS and Oh WI. Human umbilical cord blood-derived mesenchymal stem cell therapy promotes functional recovery of contused rat spinal cord through enhancement of endogenous cell proliferation and oligogenesis. J Biomed Biotechnol 2012; 2012: 362473.

[4] El-Kheir WA, Gabr H, Awad MR, Ghannam O, Barakat Y, Farghali HA, El Maadawi ZM, Ewes I and Sabaawy HE. Autologous bone marrow-derived cell therapy combined with physical therapy induces functional improvement in chronic spinal cord injury patients. Cell Transplant 2014; 23: 729-745.

[5] Boyd JG, Doucette R and Kawaja MD. Defining the role of olfactory ensheathing cells in facilitating axon remyelination following damage to the spinal cord. FASEB J 2005; 19: 694-703.

[6] Golden KL, Pearse DD, Blits B, Garg MS, Oudega M, Wood PM and Bunge MB. Transduced Schwann cells promote axon growth and myelination after spinal cord injury. Exp Neurol 2007; 207: 203-217.

[7] Hui SP, Nag TC and Ghosh S. Characterization of proliferating neural progenitors after spinal cord injury in adult zebrafish. PLoS One 2015; 10: e0143595.

[8] Menezes K, Nascimento MA, Goncalves JP, Cruz AS, Lopes DV, Curzio B, Bonamino M, de Menezes JR, Borojevic R, Rossi MI and Coelho-Sampaio T. Human mesenchymal cells from adipose tissue deposit laminin and promote regeneration of injured spinal cord in rats. PLoS One 2014; 9: e96020.

[9] All AH, Gharibani P, Gupta S, Bazley FA, Pashai N, Chou BK, Shah S, Resar LM, Cheng L, Gearhart JD and Kerr CL. Early intervention for spinal cord injury with human induced pluripotent stem cells oligodendrocyte progenitors. PLoS One 2015; 10: e0116933.

[10] Neirinckx V, Cantinieaux D, Coste C, Rogister B, Franzen R and Wislet-Gendebien S. Concise review: spinal cord injuries: how could adult mesenchymal and neural crest stem cells take up the challenge? Stem Cells 2014; 32: 829-843.

[11] Pekovic V and Hutchison CJ. Adult stem cell maintenance and tissue regeneration in the ageing context: the role for A-type lamins as intrinsic modulators of ageing in adult stem cells and their niches. J Anat 2008; 213: 5-25.

[12] Chong PP, Selvaratnam L, Abbas AA and Kamarul T. Human peripheral blood derived mesenchymal stem cells demonstrate similar characteristics and chondrogenic differentiation potential to bone marrow derived mesenchymal stem cells. J Orthop Res 2012; 30: 634-642.

[13] Tondreau T, Meuleman N, Delforge A, Dejeneffe M, Leroy R, Massy M, Mortier C, Bron D and Lagneaux L. Mesenchymal stem cells derived from CD133-positive cells in mobilized peripheral blood and cord blood: proliferation, Oct4 expression, and plasticity. Stem Cells 2005; 23: 1105-1112.

[14] Kim J, Shin JM, Jeon YJ, Chung HM and Chae JI. Proteomic validation of multifunctional molecules in mesenchymal stem cells derived from human bone marrow, umbilical cord blood and peripheral blood. PLoS One 2012; 7: e32350.

[15] Niu CC, Lin SS, Yuan LJ, Chen LH, Pan TL, Yang CY, Lai PL and Chen WJ. Identification of mesenchymal stem cells and osteogenic factors in bone marrow aspirate and peripheral blood for spinal fusion by flow cytometry and proteomic analysis. J Orthop Surg Res 2014; 9: 32.

[16] Kassis I, Zangi L, Rivkin R, Levdansky L, Samuel S, Marx G and Gorodetsky R. Isolation of mesenchymal stem cells from G-CSF-mobilized human peripheral blood using fibrin microbeads. Bone Marrow Transplant 2006; 37: 967-976.

[17] Salem HK and Thiemermann C. Mesenchymal stromal cells: current understanding and clinical status. Stem Cells 2010; 28: 585-596.

[18] Fu WL, Zhou CY and Yu JK. A new source of mesenchymal stem cells for articular cartilage repair: MSCs derived from mobilized peripheral blood share similar biological characteristics in vitro and chondrogenesis in vivo as MSCs from bone marrow in a rabbit model. Am J Sports Med 2014; 42: 592-601.

[19] Zheng RC, Park YK, Kim SK, Cho J, Heo SJ, Koak JY, Lee SJ, Park JM, Lee JH and Kim JH. Bone regeneration of blood-derived stem cells within dental implants. J Dent Res 2015; 94: 1318-1325.

[20] Li S, Huang KJ, Wu JC, Hu MS, Sanyal M, Hu M, Longaker MT and Lorenz HP. Peripheral blood-derived mesenchymal stem cells: candidate cells responsible for healing critical-sized calvarial bone defects. Stem Cells Transl Med 2015; 4: 359-368.

[21] Ukai R, Honmou O, Harada K, Houkin K, Hamada H and Kocsis JD. Mesenchymal stem cells derived from peripheral blood protects against ischemia. J Neurotrauma 2007; 24: 508-520.

[22] Chen T, Chen D, Li F and Tan Z. Netrin-1 with stem cells promote angiogenesis in limb ischemic rats. J Surg Res 2014; 192: 664-669.

[23] Nichols JE, Niles JA, DeWitt D, Prough D, Parsley M, Vega S, Cantu A, Lee E and Cortiella J. Neurogenic and neuro-protective potential of a

novel subpopulation of peripheral blood-derived CD133+ABCG2+CXCR4+ mesenchymal stem cells: development of autologous cell-based therapeutics for traumatic brain injury. Stem Cell Res Ther 2013; 4: 3.

[24] Fu Q, Zhang Q, Jia LY, Fang N, Chen L, Yu LM, Liu JW and Zhang T. Isolation and characterization of rat mesenchymal stem cells derived from granulocyte colony-stimulating factor-mobilized peripheral blood. Cells Tissues Organs 2016; [Epub ahead of print].

[25] Fu Q, Tang NN, Zhang Q, Liu Y, Peng JC, Fang N, Yu LM, Liu JW and Zhang T. Preclinical study of cell therapy for osteonecrosis of the femoral head with allogenic peripheral blood-derived mesenchymal stem cells. Yonsei Med J 2016; 57: 1006-1015.

[26] Basso DM, Beattie MS and Bresnahan JC. Graded histological and locomotor outcomes after spinal cord contusion using the NYU weight-drop device versus transection. Exp Neurol 1996; 139: 244-256.

[27] Rivlin AS and Tator CH. Objective clinical assessment of motor function after experimental spinal cord injury in the rat. J Neurosurg 1977; 47: 577-581.

[28] Ek CJ, Habgood MD, Dennis R, Dziegielewska KM, Mallard C, Wheaton B and Saunders NR. Pathological changes in the white matter after spinal contusion injury in the rat. PLoS One 2012; 7: e43484.

[29] Fang CB, Zhou DX, Zhan SX, He Y, Lin Z, Huang C and Li J. Amelioration of experimental autoimmune uveitis by leflunomide in Lewis rats. PLoS One 2013; 8: e62071.

[30] Yi J, Wang D, Niu X, Hu J, Zhou Y and Li Z. MicroRNA-155 deficiency suppresses Th17 cell differentiation and improves locomotor recovery after spinal cord injury. Scand J Immunol 2015; 81: 284-290.

[31] Mills KH. Regulatory T cells: friend or foe in immunity to infection? Nat Rev Immunol 2004; 4: 841-855.

[32] Ma K, Fox L, Shi G, Shen J, Liu Q, Pappas JD, Cheng J and Qu T. Generation of neural stem cell-like cells from bone marrow-derived human mesenchymal stem cells. Neurol Res 2011; 33: 1083-1093.

[33] Honma T, Honmou O, Iihoshi S, Harada K, Houkin K, Hamada H and Kocsis JD. Intravenous infusion of immortalized human mesenchymal stem cells protects against injury in a cerebral ischemia model in adult rat. Exp Neurol 2006; 199: 56-66.

[34] Neuhuber B, Timothy Himes B, Shumsky JS, Gallo G and Fischer I. Axon growth and recovery of function supported by human bone marrow stromal cells in the injured spinal cord exhibit donor variations. Brain Res 2005; 1035: 73-85.

[35] Veeravalli KK, Dasari VR, Tsung AJ, Dinh DH, Gujrati M, Fassett D and Rao JS. Human umbilical cord blood stem cells upregulate matrix metalloproteinase-2 in rats after spinal cord injury. Neurobiol Dis 2009; 36: 200-212.

[36] Nandoe Tewarie RD, Hurtado A, Levi AD, Grotenhuis JA and Oudega M. Bone marrow stromal cells for repair of the spinal cord: towards clinical application. Cell Transplant 2006; 15: 563-577.

[37] Liu XH, Zhang T, Zhang Q, Liu JW, Liu ZI, Tang NN. Colony froming capacity and neuron differentiation of rabbit peripheral blood-derived mesenchymal stem cells after G-CSF mobilization. Journal of Xi'an Jiaotong University (Medical Sciences) 2014; 35: 26-29.

[38] Sakamoto Y, Kitamura K, Yoshimura K, Nishijima T and Uyemura K. Complete amino acid sequence of PO protein in bovine peripheral nerve myelin. J Biol Chem 1987; 262: 4208-4214.

[39] Deber CM and Reynolds SJ. Central nervous system myelin: structure, function, and pathology. Clin Biochem 1991; 24: 113-134.

[40] Jacque CM, Vinner C, Kujas M, Raoul M, Racadot J and Baumann NA. Determination of glial fibrillary acidic protein (GFAP) in human brain tumors. J Neurol Sci 1978; 35: 147-155.

[41] Tardy M, Fages C, Le Prince G, Rolland B and Nunez J. Regulation of the glial fibrillary acidic protein (GFAP) and of its encoding mRNA in the developing brain and in cultured astrocytes. Adv Exp Med Biol 1990; 265: 41-52.

[42] Weinstein DE, Shelanski ML and Liem RK. Suppression by antisense mRNA demonstrates a requirement for the glial fibrillary acidic protein in the formation of stable astrocytic processes in response to neurons. J Cell Biol 1991; 112: 1205-1213.

[43] Lever IJ, Robinson M, Cibelli M, Paule C, Santha P, Yee L, Hunt SP, Cravatt BF, Elphick MR, Nagy I and Rice AS. Localization of the endocannabinoid-degrading enzyme fatty acid amide hydrolase in rat dorsal root ganglion cells and its regulation after peripheral nerve injury. J Neurosci 2009; 29: 3766-3780.

[44] Dawson DA and Hallenbeck JM. Acute focal ischemia-induced alterations in MAP2 immunostaining: description of temporal changes and utilization as a marker for volumetric assessment of acute brain injury. J Cereb Blood Flow Metab 1996; 16: 170-174.

[45] Ekmark-Lewen S, Lewen A, Israelsson C, Li GL, Farooque M, Olsson Y, Ebendal T and Hillered L. Vimentin and GFAP responses in astrocytes after contusion trauma to the murine brain. Restor Neurol Neurosci 2010; 28: 311-321.

[46] Vos PE, Jacobs B, Andriessen TM, Lamers KJ, Borm GF, Beems T, Edwards M, Rosmalen CF

and Vissers JL. GFAP and S100B are biomarkers of traumatic brain injury: an observational cohort study. Neurology 2010; 75: 1786-1793.

[47] Abrams MB, Dominguez C, Pernold K, Reger R, Wiesenfeld-Hallin Z, Olson L and Prockop D. Multipotent mesenchymal stromal cells attenuate chronic inflammation and injury-induced sensitivity to mechanical stimuli in experimental spinal cord injury. Restor Neurol Neurosci 2009; 27: 307-321.

[48] Dasari VR, Spomar DG, Gondi CS, Sloffer CA, Saving KL, Gujrati M, Rao JS and Dinh DH. Axonal remyelination by cord blood stem cells after spinal cord injury. J Neurotrauma 2007; 24: 391-410.

[49] Nakajima H, Uchida K, Guerrero AR, Watanabe S, Sugita D, Takeura N, Yoshida A, Long G, Wright KT, Johnson WE and Baba H. Transplantation of mesenchymal stem cells promotes an alternative pathway of macrophage activation and functional recovery after spinal cord injury. J Neurotrauma 2012; 29: 1614-1625.

[50] Zhou L, Lopes JE, Chong MM, Ivanov, II, Min R, Victora GD, Shen Y, Du J, Rubtsov YP, Rudensky AY, Ziegler SF and Littman DR. TGF-beta-induced Foxp3 inhibits T(H)17 cell differentiation by antagonizing RORgammat function. Nature 2008; 453: 236-240.

[51] Mangan PR, Harrington LE, O'Quinn DB, Helms WS, Bullard DC, Elson CO, Hatton RD, Wahl SM, Schoeb TR and Weaver CT. Transforming growth factor-beta induces development of the T(H)17 lineage. Nature 2006; 441: 231-234.

[52] Kolls JK and Linden A. Interleukin-17 family members and inflammation. Immunity 2004; 21: 467-476.

[53] Janke M, Peine M, Nass A, Morawietz L, Hamann A and Scheffold A. In-vitro-induced Th17 cells fail to induce inflammation in vivo and show an impaired migration into inflamed sites. Eur J Immunol 2010; 40: 1089-1098.